



NUMERICAL MODELING OF VENTURI FLOWS FOR DETERMINING AIR INJECTION RATES USING FLUENT V6.2

Ahmet Baylar^{*}, M. Cihan Aydin^{**}, Mehmet Unsal^{***} and Fahri Ozkan^{***}

^{*} Firat University, Civil Engineering Department, Elazig, Turkey, abaylar@firat.edu.tr

^{**} Yuzuncu Yil University, Technical Vocational School of Higher Education, Bitlis, Turkey

^{***} Firat University, Construction Education Department, Elazig, Turkey

Abstract- As the water passes through a restriction in a pipe, it forms a vacuum at the end of the restriction. A hole bored into the pipe at a point where this vacuum occurs will cause air to be drawn into the main flow. One example of this mechanism is seen in the venturi tube. When a minimal amount of differential pressure exists between the inlet and outlet sides of the venturi tube, a vacuum occurs at suction holes of the venturi tube. Venturi aeration is a method of aeration that has become popular in recent years. In present paper, air injection rates of venturi tubes are analyzed using Computational Fluid Dynamics modeling. These analyses are carried out by means of the program FLUENT V6.2 that uses finite volume theory. There is a good agreement between the measured air injection rates and the values computed from FLUENT CFD program.

Keywords- Aeration, Air injection, Computational Fluid Dynamics, Venturi.

1. INTRODUCTION

The ecological quality of water depends largely on the amount of oxygen that water holds. The higher the level of dissolved oxygen the better the quality of water system. By measuring dissolved oxygen, scientists determine the quality of water and healthiness of an ecosystem. Oxygen enters water by entrainment of air bubbles. Many industrial and environmental processes involve the aeration of a liquid by the entrainment of air bubbles.

Venturi aeration is one of the ideal forms to increase air entrainment and oxygen content in water body for hydraulic and environmental engineering. When a minimal amount of differential pressure exists between the inlet and outlet sides of the venturi tube, a vacuum (air suction) occurs at suction holes of the venturi tube (Fig. 1). When a pressurized operating (motive) fluid, such as water, enters the venturi tube inlet, it constricts toward the throat portion of the venturi tube and changes into a high velocity jet stream. The increase in velocity through the throat portion of the venturi tube, as a result of the differential pressure, results in a decrease in pressure in the throat portion. This pressure drop enables air to be injected through the suction holes and is dynamically entrained into the motive stream. As the jet stream is diffused toward the venturi tube outlet, velocity is reduced and reconverted into pressure energy (but at a level lower than the venturi tube inlet pressure). Venturi tubes are high efficient, requiring less than 20 % differential to initiate suction.

There are many advantages of using venturi tubes in the water aeration systems. The venturi tube does not require external power to operate. It does not have any moving parts, which increases its life and decreases probability of failure. The venturi

tube is usually constructed of plastic and it is resistant to most chemicals. It requires minimal operator attention and maintenance. Since the device is very simple, its cost is low as compared to other equipment of similar function and capability. It is easy to adapt to most of new or existing systems providing that there is sufficient pressure in the system to create the required pressure differential. Because the venturi tube utilizes a vacuum principle rather than a pressure principle, the material being handled is never under high pressure in a concentrated form. This reduces the possibility of caustic chemicals being sprayed into the air through cracks or breaks in the pipe.

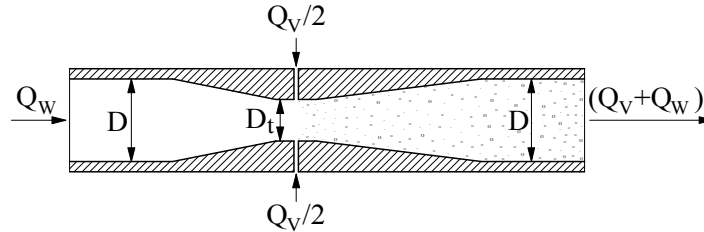


Figure 1. Air Suction Produced by Venturi Tube

Recently, Baylar and Emiroglu [1], Emiroglu and Baylar [2], Baylar et al. [3], Baylar and Ozkan [4], Ozkan et al. [5] and Baylar et al. [6, 7] studied the use of venturi tubes in water aeration systems. All of these works were experimental and none concentrated specifically on Computational Fluid Dynamics (CFD) modeling of venturi tubes. In this study, air injection rates of venturi tubes are analyzed using CFD modeling.

2. AIR INJECTION MECHANISM IN VENTURI TUBE

The converging tube is an effective device for converting pressure head to velocity head, while the diverging tube converts velocity head to pressure head. The two may be combined to form a venturi tube, named after Venturi, an Italian, who investigated its principle about 1791. It was applied to the measurement of water by Clemens Herschel in 1886. As shown in Fig. 2, it consists of a tube with a constricted throat which produces an increased velocity accompanied by a reduction in pressure, followed by a gradually diverging portion in which the velocity is transformed back into pressure with slight friction loss.

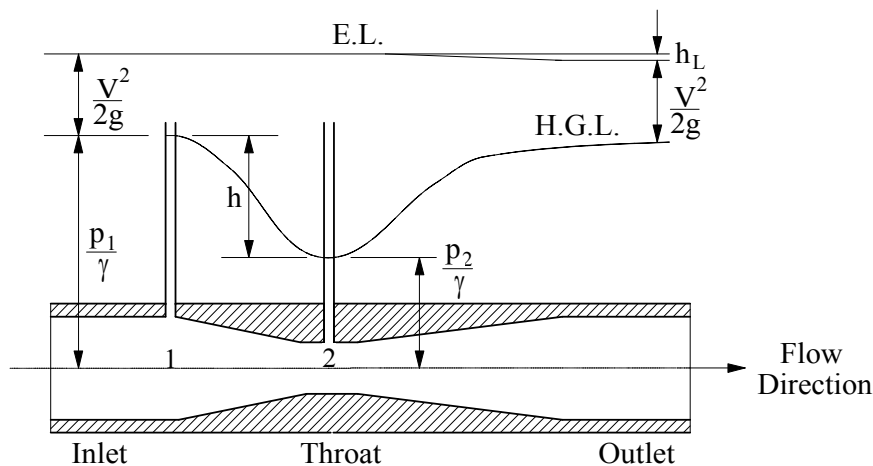


Figure 2. Definition Sketch for Venturi Tube [8]

Writing the Bernoulli equation between section 1 and 2 of Fig. 2, we have, for the ideal case,

$$\frac{p_1}{\gamma} + z_1 + \frac{V_1^2}{2g} = \frac{p_2}{\gamma} + z_2 + \frac{V_2^2}{2g} \quad (1)$$

where 1 and 2 are subscripts indicating points 1 and 2; p_1 and p_2 are pressures; γ is specific weight; z_1 and z_2 are elevations; V_1 and V_2 are velocities and g is gravitational acceleration.

Since $z_1 = z_2$, Equation 1 may be written

$$\frac{p_2}{\gamma} = \frac{p_1}{\gamma} + \frac{V_1^2}{2g} - \frac{V_2^2}{2g} \quad (2)$$

Applying the continuity equation to points 1 and 2 allows us to express the flow velocity at point 1 as a function of the flow velocity at point 2 and the ratio of the two flow areas

$$V_1 = \left(\frac{A_2}{A_1} \right) V_2 = \beta V_2 \quad (3)$$

where A_1 and A_2 is flow areas in points 1 and 2 and β is ratio of throat flow area of the venturi tube to inlet flow area of the venturi tube.

Substituting this value into Equation 2

$$\frac{p_2}{\gamma} = \frac{p_1}{\gamma} + \frac{V_2^2(\beta^2 - 1)}{2g} \quad (4)$$

The venturi effect happens due to pressure drop in the throat portion as velocity in the throat portion increases. The increase in velocity V_2 through the throat portion of the venturi tube, as a result of the differential pressure, results in a decrease in pressure p_2 in the throat portion. When the pressure p_2 in the throat portion drops under atmospheric pressure ($p_2 < p_{atm}$), air is injected through suction holes and is dynamically entrained into the motive stream.

3. EXPERIMENTAL APPARATUS AND PROCEDURES

Experimental investigations were conducted by Baylar et al. [6] using the experimental setup in the Hydraulic Research Laboratory, Civil Engineering Department, Firat University, Elazig, Turkey. In this study, data are taken from Baylar et al. [6]. The detail of experimental setup and procedure is given below.

3.1. Experimental Setup

General view of the experimental setup is given in Fig. 3. The experimental setup consisted of water tank, water pump, flow control valve, water flowmeter, water feed line, venturi tube, air hood and release valve. All experiments were carried out in a 1.8 m³ water tank with glass-walls (0.75 m wide x 2.0 m long x 1.2 m high). The water in the experimental set-up was circulated by a water pump through a water flowmeter.

The venturi tubes used in experiments were manufactured in clear plastic material. The inlet and outlet diameters of the venturi tubes, D , were 36 mm, 42 mm and 54 mm. The ratio of throat diameter of venturi tube to inlet diameter of venturi tube, D_t/D , was taken as 0.75. Throat length of the venturi tubes was selected as D_t . The

converging cone angle θ_1 and the diverging cone angle θ_2 of the venturi tubes were 21° and 7° , respectively. The converging cone angle of 21° and the diverging cone angle of 7° are those that, according to the American Society of Mechanical Engineers [9], minimize the head losses for the venturi tube. At the throat portion of the venturi tubes, two holes with diameter of 6.0 mm were drilled through the wall.

3.2. Experimental Procedure

Baylar et al. [6] investigated the effect of the venturi tubes with diameters of 36 mm, 42 mm and 54 mm on air injection rate, Q_V . In the flow of the fluid through a completely filled venturi tube, gravity does not affect the flow pattern. Thus, the Reynolds number was used as dimensionless parameter. The Reynolds number was varied between 35000 and 437000. When a minimal amount of differential pressure existed between the venturi inlet and outlet portions, the venturi tubes caused air to be drawn into the water stream. An air hood for which the plan-view dimensions were 0.70 m x 0.75 m, was used to trap air bubbles entering air holes on venturi tubes. Air injection rate, Q_V , was measured by using an air flowmeter (Testo Model 435 anemometer) installed on the air hood surface, as illustrated in Fig. 3.

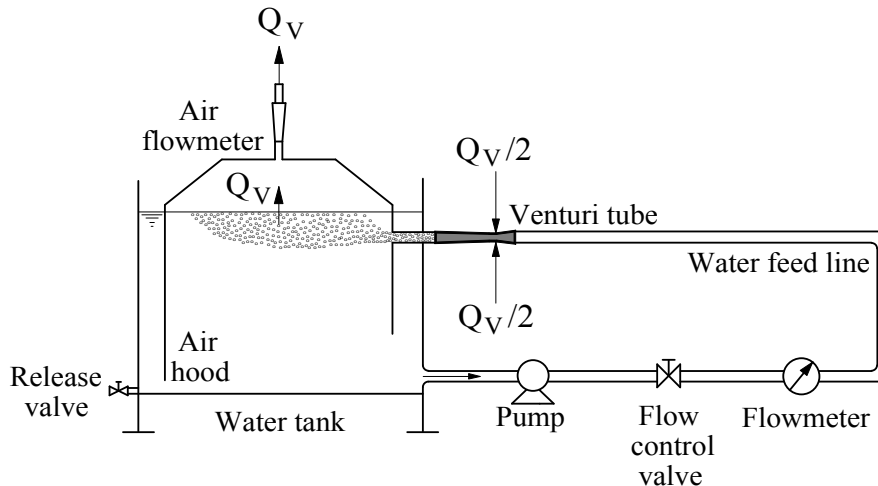


Figure 3. Schematic Representation of Venturi Tube Experimental Apparatus

4. APPLICATION OF CFD MODELLING TO VENTURI TUBES

CFD (Computational Fluid Dynamics) is a technique for solving the equations that govern fluid flow on computers. This technique has become so important that it now occupies the attention of perhaps a third of all researchers in fluid mechanics and the proportion is still increasing [10]. One of the reasons for its popularity is that it can be used to solve real world problems. Solving the equations for fluid flow exactly is almost always impossible, except in some special cases. In CFD, the equations of fluid flow have to be discretized, which means that the domain of interest (e.g. the air surrounding a car or the water inside a turbine) has to be subdivided into small elements (together they are called the grid or the mesh). This also means that the solution (the velocity, pressure, etc.) is not available in the entire flow domain but only at each element. It is important to understand that a CFD solution to a particular problem

involves approximations at several levels. The equations being solved are a model of reality, not reality itself. Secondly, when the equations are discretized, approximations are introduced. If it was possible to use an infinite number of elements it would be possible to get very close to the exact solution. But since computers are not infinite fast with infinite memory, there is a limit on the number of elements that can be used. Therefore we can not resolve everything inside the flowing fluid. The actual CFD solving process is often done in steps (iterations) towards the exact solution. This process has to be stopped at some level which means that the exact solution to the discretized equations is never reached (but it is possible to get very close) [10].

In this study, using Computational Fluid Dynamics (CFD) modeling, the air injection rates of venturi tubes are analyzed. These analyses are carried out by means of FLUENT V6.2 program. FLUENT is a Computational Fluid Dynamics software package to simulate fluid flow problems. It uses the finite-volume method to solve the governing equations for a fluid. It provides the capability to use different physical models such as incompressible or compressible, inviscid or viscous, laminar or turbulent, etc.

4.1. Solution Strategies

In the numerical solutions, 3D multiphase model (Algebraic Slip Mixture Model) and standard k- ϵ turbulence model are used. The standard k- ϵ model is a semi-empirical model based on model transport equations for the turbulence kinetic energy (k) and its dissipation rate (ϵ) [11]. The model transport equation for k is derived from the exact equation, while the model transport equation for ϵ is obtained using physical reasoning and bears little resemblance to its mathematically exact counterpart.

The algebraic slip mixture model is used in the numerical solutions with FLUENT V6.2 CFD program. The algebraic slip mixture model does not assume that there is an interface between two immiscible phases; it allows the phases to be interpenetrating. Moreover, the algebraic slip mixture model allows the two phases to move at different velocities. The algebraic slip mixture model can solve the continuity equation and the momentum equation for the mixture [12].

The continuity equation for the mixture is

$$\frac{\partial}{\partial t}(\rho_m) + \frac{\partial}{\partial x_i}(\rho_m u_{m,i}) = 0 \quad (5)$$

where ρ_m is mixture density and \bar{u}_m is mass-averaged velocity. No mass transfer is allowed in the algebraic slip mixture model.

The momentum equation for the mixture can be obtained by summing the individual momentum equations for both phases. It can be expressed as

$$\begin{aligned} \frac{\partial}{\partial t} \rho_m u_{m,j} + \frac{\partial}{\partial x_i} \rho_m u_{m,i} u_{m,j} = \\ - \frac{\partial p}{\partial x_j} + \frac{\partial}{\partial x_i} \mu_m \left(\frac{\partial u_{m,i}}{\partial x_j} + \frac{\partial u_{m,j}}{\partial x_i} \right) + \rho_m g_j + F_j + \frac{\partial}{\partial x_i} \sum_{k=1}^n \alpha_k \rho_k u_{Dk,i} u_{Dk,j} \end{aligned} \quad (6)$$

where n is number of phases; μ_m is viscosity of mixture; F is a body force; α_k is volume fraction of phase k and \bar{u}_{Dk} is drift velocity.

The boundary conditions in the numerical model are defined as velocity inlet (water inlet), pressure inlets (air inlet with atmospheric pressure), walls (solid surfaces), and outlet (water and air outlet) as shown Fig. 4.

4.2. Boundary Conditions

The velocity inlet boundary condition is applied to determine the water flow rate at the entry of venturi tube. The water velocities of the boundary are changed from 1.0 m/s to 8.75 m/s, so the water discharges, Q_w , are taken into account as the range from $1.02 \times 10^{-3} \text{ m}^3/\text{s}$ to $18.70 \times 10^{-3} \text{ m}^3/\text{s}$. The pressure inlet and the outflow are applied to the boundary of air inlet nozzle and the boundary of exit of venturi, respectively (Fig.4). The pressure values in the boundary of pressure inlet and outflow are chosen as zero Pascal.

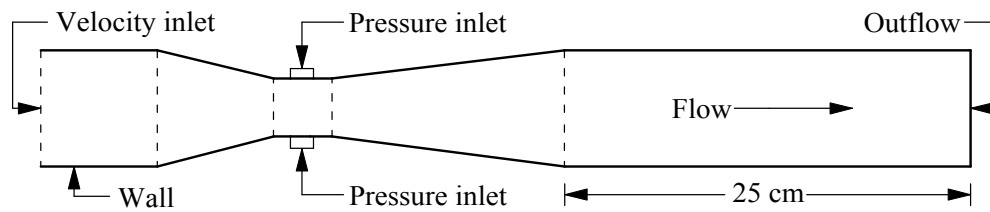


Figure 4. Boundary conditions of the numerical model

In velocity inlet of boundary,

$$U_n = U_w \quad (7)$$

where U_n is velocity normal to boundary (m/s) and U_w is mean water velocity (m/s).

Therefore, the water discharge of the venturi tube is defined as:

$$Q_w = U_n A \quad (8)$$

where A is cross section area of venturi tube with diameter of D .

In this study, the turbulence intensity, I , and the hydraulic diameter are defined as turbulence parameters in the boundary conditions for $k-\epsilon$ turbulence model. The turbulence intensity, I , is defined as the ratio of the root-mean-square of the velocity fluctuations, to the mean flow velocity. A turbulence intensity of 1% or less is generally considered low and turbulence intensities greater than 10% are considered high. The turbulence intensity at the core of a fully-developed duct flow can be estimated from the following formula derived from an empirical correlation for pipe flows [12]

$$I = 0.16(\text{Re})^{-1/8} \quad (9)$$

At a Reynolds Number of 50,000, for example, the turbulence intensity will be 4%, according to Equation 9. In this study, generally, the turbulence intensity is estimated between 3%-5%, since the range of Reynolds Numbers is 35000-437000.

The relationship between the turbulent kinetic energy, k , and turbulence intensity, I , is

$$k = \frac{3}{2}(u_{\text{avg}} I)^2 \quad (10)$$

where u_{avg} is mean flow velocity.

If the turbulence length scale, l , is known, turbulence dissipation rate, ε , can be determined from the following relationship

$$\varepsilon = C_{\mu}^{3/4} \frac{k^{3/2}}{l} \tag{11}$$

where C_{μ} is an empirical constant specified in turbulence model (approximately 0.09).

The turbulence length scale, l , is a physical quantity related to the size of the large eddies that contain the energy in turbulent flows. In fully-developed duct flows, l is restricted by the size of the duct, since the turbulent eddies cannot be larger than the duct. An approximate relationship between l and the physical size of the duct is

$$l = 0.07L \tag{12}$$

where L is the relevant dimension of the duct. The factor of 0.07 is based on the maximum value of the mixing length in fully-developed turbulent pipe flow, where L is the diameter of the pipe. In a channel of non-circular cross-section, L can be based on the hydraulic diameter.

4.3. Grid and Iterative Convergences

Geometry and grid generation is done using GAMBIT [13] which is the preprocessor bundled with FLUENT. In this study, the numerical model geometries are prepared with GAMBIT program and are divided into between 270,000 with 914,000 hexahedral/hybrid elements (Fig. 5). The fine and coarse grids are applied in the flow domain and the convergence and stability of the solution are found to be insensitive to the grid size in the main body of the flow.

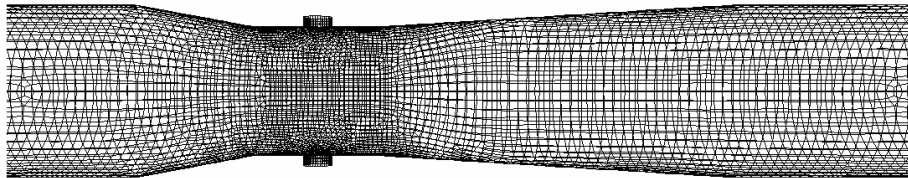


Figure 5. Meshed view of Computational Domain of Venturi Tube for D=36 mm

In the iterative solutions, it must be ensured that iterative convergence is achieved with at least three orders of magnitude decrease in the normalized residuals for each equation solved. For time-dependent problems, iterative convergences at every time step are checked and all residuals are dropped below four orders (10^{-4}) in about 300 time steps (6,000 iterations). The time steps size are selected as $t=0.01s$. Iterative convergence is achieved in about 350 time steps (7,000 iterations).

5. RESULTS

Using Computational Fluid Dynamics (CFD) modeling, the air injection rates of the venturi tubes are analyzed. These analyses are performed by means of the program FLUENT V6.2 that uses finite volumes theory. Figs. 6-10 present the aeration mechanism of the venturi tubes for water inlet velocity, U_w , of 8.75 m/s in the diameters of 36, 42 and 54 mm. In Fig. 6 (a-c), the static pressure distribution on the sections show that static pressure decreases at the throat portion. In this figure, it is seen that the pressure at the right of the air suction hole decreases extremely. As shown Fig. 7, at this small region, the air entrainment is maximum and the air entrainment velocity, U_a ,

greater than 40 m/s (up to 100 m/s). Simultaneously, Fig. 9 shows that an intense turbulent occurs at the same region. The turbulent intensity dissolves away from this region. Again at the end corner of converging cone, the pressure drops too. It is pointed out that this region, owing to also no exist any air mixture, can generate cavitation.

In Figs. 6 and 7, as expected, the increasing of flow velocity at the throat portion accompanied by reduction in the pressure can be seen clearly. Furthermore, it is seen in Fig.6 that the static pressure before the converging cone decreases with increasing of the diameters of venturi and throat, while the negative pressure in the throat do not change too much with increasing diameter.

The distribution of volume fraction of air phase on the lengthwise section is presented with equal-lines in Fig. 8. For $D=36$ mm, the clear water core (no air) in flow domain after suction holes almost continues at the end of diverging cone center (Fig. 8a) but for bigger diameters this clear water region is longer. As seen in Fig. 8, the bigger diameter constitutes longer clear water core on the venturi center line. Therefore, the venturi length required to provide fully aerated cross-sectional area can be defined by considering the volume fractions as shown in Fig. 8.

The velocity lines and velocity vectors of the mixture are given in Figs. 7 and 10 for the different diameters of venturi. In these figures, it is seen that the velocity magnitudes in sections do not change too much with changing venturi diameters. Turbulence intensities given in Fig. 9 develop toward downstream with increasing diameter.

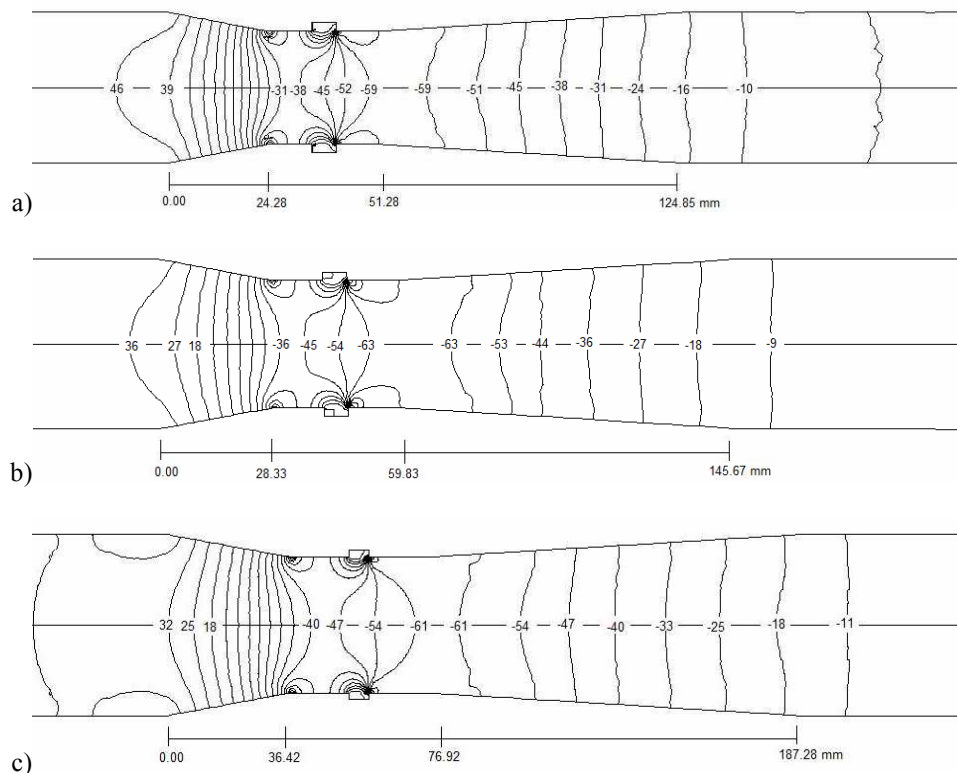


Figure 6. Static Pressure Distribution of Section for $U_w=8.75$ m/s: a) $D=36$ mm, $D_t=27$ mm; b) $D=42$ mm, $D_t=31.5$ mm; c) $D=54$ mm, $D_t=40.5$ mm ($P_{\max} = 46$ KPa, $P_{\min} = -107.73$ KPa)

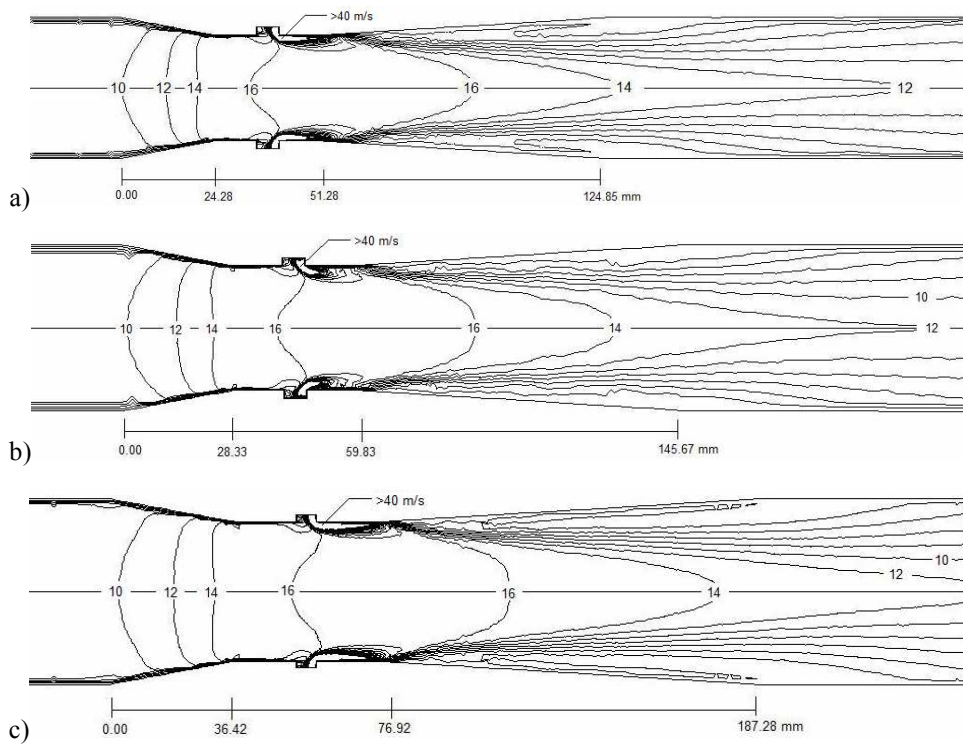


Figure 7. Contours of Velocity Magnitude (m/s) of Mixture for $U_w=8.75$ m/s:
 a) $D=36$ mm, $D_i=27$ mm; b) $D=42$ mm, $D_i=31.5$ mm; c) $D=54$ mm, $D_i=40.5$ mm

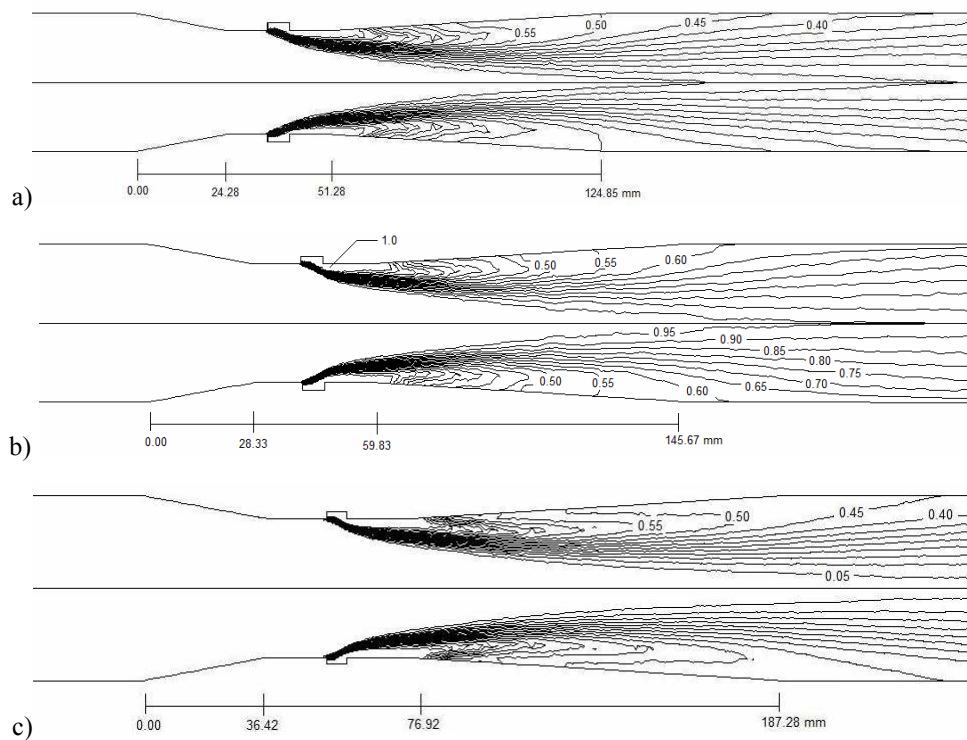


Figure 8. Contours of Volume Fraction of Air for $U_w=8.75$ m/s: a) $D=36$ mm, $D_i=27$ mm; b) $D=42$ mm, $D_i=31.5$ mm; c) $D=54$ mm, $D_i=40.5$ mm (The range of the line values is 0 - 1)

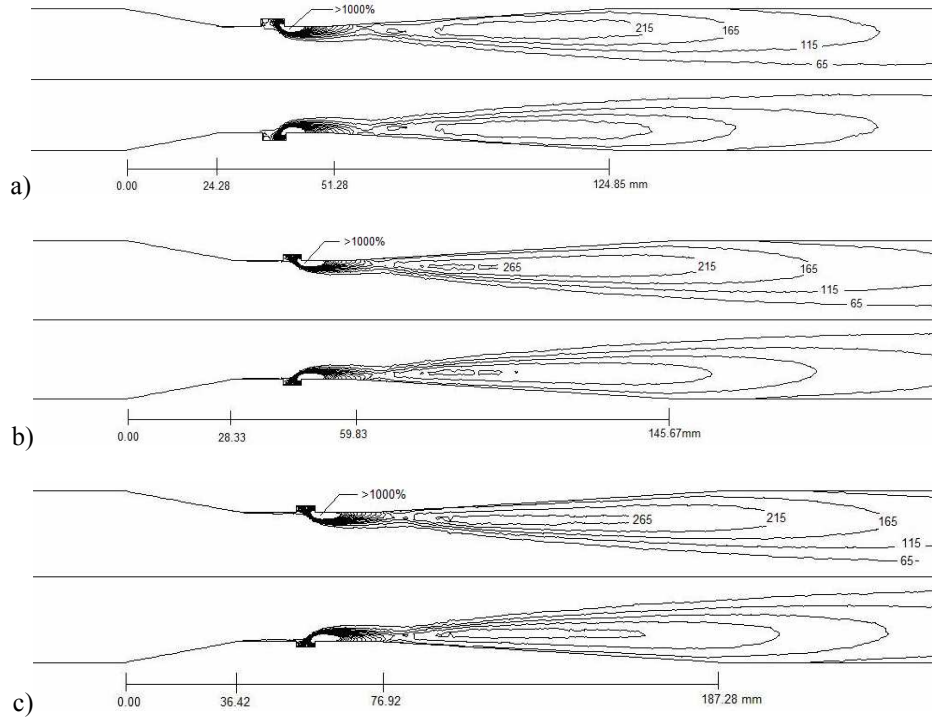


Figure 9. Contours of Turbulence Intensity for $U_w=8.75$ m/s: a) $D=36$ mm, $D_i=27$ mm; b) $D=42$ mm, $D_i=31.5$ mm; c) $D=54$ mm, $D_i=40.5$ mm (The equal-line values change from 65% to 1000%)

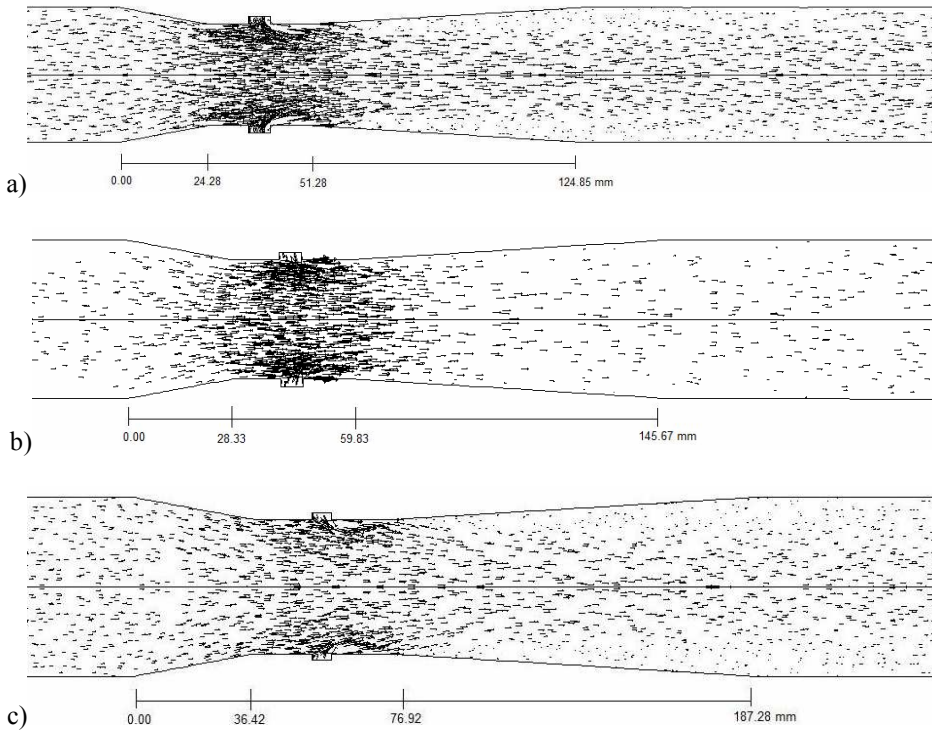


Figure 10. Velocity Vectors for $U_w=8.75$ m/s: a) $D=36$ mm, $D_i=27$ mm; b) $D=42$ mm, $D_i=31.5$ mm; c) $D=54$ mm, $D_i=40.5$ mm (The values of vectors change from 0 m/s to 50 m/s)

Moreover, the values computed from FLUENT V6.2 CFD program are compared with Baylar et al.'s [6] experimental laboratory results, as shown in Fig. 11. The experimental results and those obtained with FLUENT V6.2 CFD program have good agreement with each other. The mean rates of errors between the experimental and the CFD results in Figs. 11 a, b and c are 12%, 6% and 13%, respectively. These errors can result from such things as selected turbulence and mathematical model, disregarding environment conditions, grid size in numerical models and measurement faults in the laboratory tests.

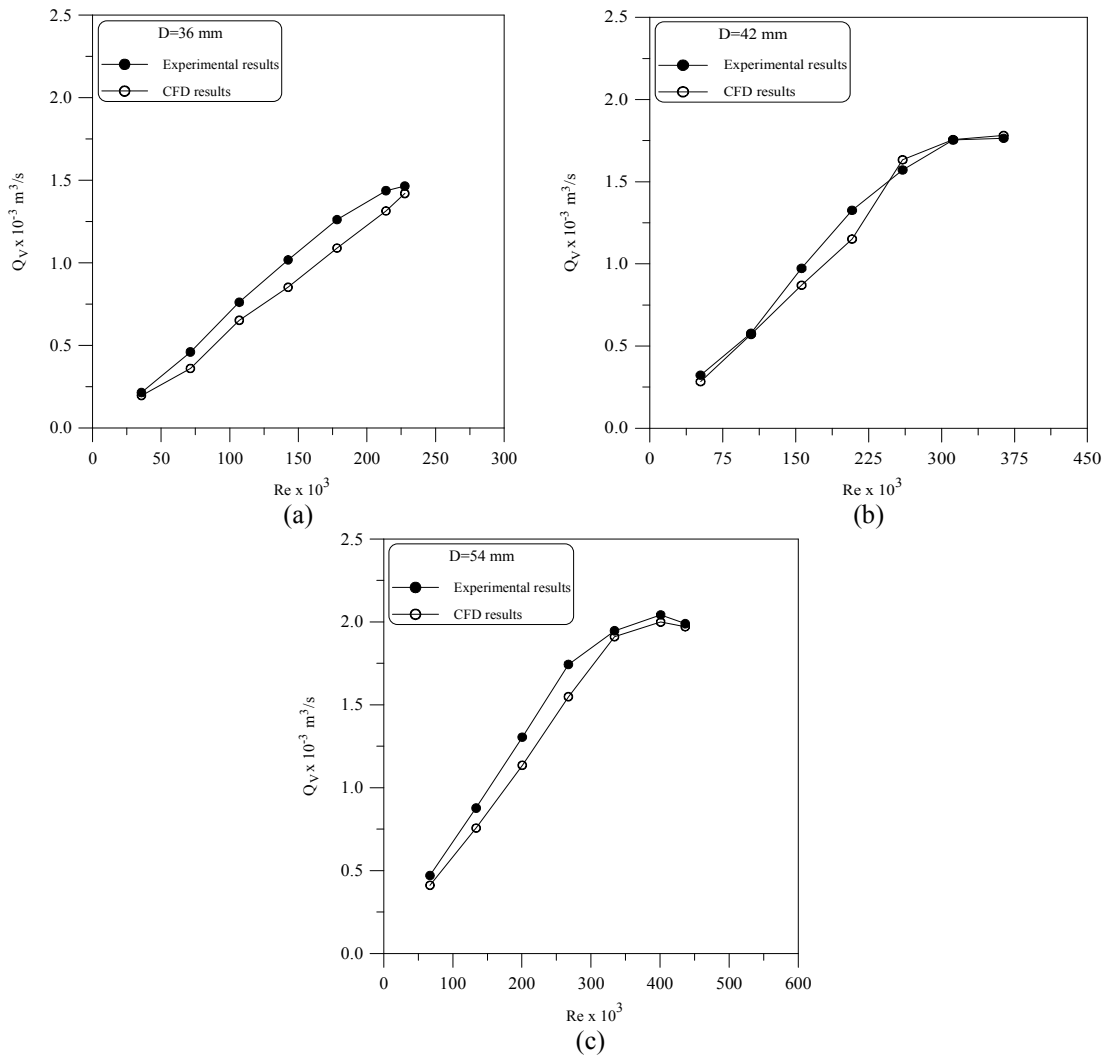


Figure 11. Plot of Q_v versus Re for Experimental and CFD Results for a) D=36 mm, b) D=42 mm, c) D=54 mm

6. CONCLUSIONS

Many industrial and environmental processes involve the aeration of a liquid by the entrainment of air bubbles. Venturi aeration is a particular instance of this, and the aeration properties of venturies have been studied widely over a number of years. In this study, air injection rates of venturi tubes are analyzed using Computational Fluid

Dynamics modeling. These analyses are carried out by means of FLUENT V6.2 CFD program that uses finite-volume method. The following conclusions can be presented depending on CFD analyses:

- I. The results obtained from CFD analyses will lead air suction mechanism of a venturi to be understood better.
- II. There is a good agreement between the measured air injection rates and the values computed from FLUENT V6.2 CFD program. Therefore, CFD analyses can be used to determine optimum dimensions of venturi to get higher air injection rate.
- III. The harmful effect of cavitation can be prevented by watching changes in velocity and pressure.
- IV. The pressure-velocity characteristics of venturi are not affected too much by changing of venturi and throat diameters. But the diameters affect the length of non-aerated flow region of venturi.

7. REFERENCES

- [1] A. Baylar and M. E. Emiroglu, Air entrainment and oxygen transfer in a venturi, *Proc. Instn Civ. Engrs Water and Marit. Engrg.*, **156** (WM3), 249-255, 2003.
- [2] M. E. Emiroglu and A. Baylar, Study of the influence of air holes along length of convergent-divergent passage of a venturi device on aeration, *J. Hydr. Res.*, **41** (5), 513-520, 2003.
- [3] A. Baylar, F. Ozkan and M. Ozturk, Influence of venturi cone angles on jet aeration systems, *Proc. Instn Civ. Engrs Water Management*, **158** (WM1), 9-16, 2005.
- [4] A. Baylar and F. Ozkan, Applications of venturi principle to water aeration systems, *Environmental Fluid Mechanics*, **6** (4), 341-357, 2006.
- [5] F. Ozkan, M. Ozturk and A. Baylar, Experimental investigations of air and liquid injection by venturi tubes, *Water and Environment Journal*, **20** (3), 114-122, 2006.
- [6] A. Baylar, F. Ozkan and M. Unsal, On the use of venturi tubes in aeration, *CLEAN-Soil, Air, Water*, **35** (2), 183-185, 2007.
- [7] A. Baylar, M. Unsal and F. Ozkan, Determination of the optimal location of the air hole in venturi aerators, *CLEAN-Soil, Air, Water*, **35** (3), 246-249, 2007.
- [8] R. L. Daugherty, J. B. Franzini and E. J. Finnemore, *Fluid Mechanics with Engineering Applications*, McGraw-Hill Inc., New York, 1985.
- [9] American Society of Mechanical Engineers, *Measurement of Fluid Flow in Pipes Using Orifice, Nozzle and Venturi*, ASME Standard MFC-3M-1989, Reaffirmed 1995.
- [10] J. H. Ferziger and M. Peric, *Computational Methods for Fluid Dynamics*, Springer-Verlag, Berlin, Heidelberg, 1996.
- [11] B. E. Launder and D. B. Spalding, *Lectures in Mathematical Models of Turbulence*, Academic Press, London, England, 1972.
- [12] FLUENT 6.2, *User's Guide*, FLUENT Inc., Lebanon, NH, 2005.
- [13] GAMBIT 2.2, *Modeling Guide*, FLUENT Inc., Lebanon, NH, 2005.